The Interaction of Genotype and Environment Determines Variation in the Maize Kernel Ionome

Alexandra Asaro[1], Greg Ziegler[2], Cathrine Ziyomo[1], Owen A. Hoekenga[3], Brian P. Dilkes[4], Ivan Baxter[2]*

[1]Donald Danforth Plant Science Center, St. Louis, Missouri, United States of America

[2]USDA-ARS, Donald Danforth Plant Science Center, St. Louis, Missouri, United States of America

[3]Genomics Consultant, Ithaca, New York, United States of America

[4]Department of Biochemistry, Purdue University, West Lafayette, Indiana, United States of America

*Corresponding author

E-mail: ivan.baxter@ars.usda.gov (IB)

Abstract

Plants obtain soil-resident elements that support growth and metabolism via water-mediated flow facilitated by transpiration and active transport processes. The availability of elements in the environment interact with the genetic capacity of organisms to modulate element uptake through plastic adaptive responses, such as homeostasis. These interactions should cause the elemental contents of plants to vary such that the effects of genetic polymorphisms influencing elemental accumulation will be dramatically dependent on the environment in which the plant is grown. To investigate genotype by environment interactions underlying elemental accumulation, we analyzed levels of elements in maize kernels of the Intermated B73 x Mo17 (IBM) recombinant inbred population grown in 10 different environments spanning a total of six locations and five different years. We identified quantitative trait loci controlling elemental accumulation by considering individual elemental accumulation measurements as traits and by mapping the loci responsible for variation in co-regulated multi-elemental traits identified using principle components analysis. These approaches detected partially overlapping sets of loci, many of which were found only in a single growout. We applied our multi-element approach across all of the growouts and found that the growth environment has a profound effect on the elemental profile and that some multi-element phenotypes correlate with specific environmental variables. We identified QTL by environment interactions (QEIs) through three methods: linear modeling with environmental covariates, QTL analysis on trait differences between growouts, and QTL analysis on factors obtained from a principle component derived model of ionome variation across environments. Overall, we were able to map 79 elemental QTL, 101 principal component QTL, and several instances of QEI, indicating that elemental profiles are highly heritable, interrelated, and responsive to the environment.

Author Summary

Plants take up elements from the soil, a process that is highly regulated by the plant's genome. In order to look at how maize alters its elemental uptake in response to different environments, we analyzed the kernel elemental content of a population derived from a cross grown 10 different times in six locations. We found that environment had a profound effect on which genetic loci were important for elemental accumulation in the kernel. We also found that the elements are not regulated independently and that mathematical combinations of elements will identify different genetic loci than single element approaches. The mathematical combinations of elements are correlated with environmental variables, suggesting that underlying the observed variation are interactions between genetically controlled factors and environmental variables. Our results suggest that to have a full understanding of elemental accumulation in maize kernels and other food crops, we will need to understand the interactions identified here at the level of the genes and the environmental variables that contribute to loading essential nutrients into seeds.

Introduction

The intake, transport, and storage of elements are key processes underlying plant growth and survival. A plant must balance mineral levels to prevent accumulation of toxic concentrations of elements while taking up essential elements for growth. Food crops must strike similar balances to provide healthy nutrient contents of edible tissues. Adaptation to variation in soil, water, and temperature requires that plant genomes encode flexible regulation of mineral physiology to achieve homeostasis [1]. This regulation must be responsive both to the availability of each regulated element in the environment and to the levels of these elements at the sites of use within the plant. Understanding how the genome encodes responses to element

47 limitation or toxic excess in nutrient-poor or contaminated soils will help sustain our rapidly
48 growing human population [2].
49 The concentrations of elements in a plant sample provide a useful read-out for the
50 environmental, genetic and physiological processes important for plant adaptation. We and
51 others developed high-throughput and inexpensive pipelines to detect and quantitate 20 different
52 elemental concentrations by inductively coupled plasma mass spectrometry (ICP-MS). This
53 process, termed *ionomics*, is the quantitative study of the complete set of mineral nutrients and
54 trace elements in an organism (its *ionome*) [3]. In crop plants such as maize and soybean, seed
55 element profiles make an ideal study tissue as seeds provide a read-out of physiological status of
56 the plant and are the food source.
57 There are many lines of evidence that elements covary with each other due to
58 physiological, genetic or environmental factors. For example, a suite of elements responds to Fe
59 deficiency in such a concerted manner that they can be used to predict the Fe status of the plant
60 [4]. When *A. thaliana* recombinant populations were grown in multiple environments, genetic
61 correlations among Li-Na, Mg-Ca, and Cu-Zn were observed across all environments while other
62 pairs (Ca-Fe and Mg-Fe) were only correlated in a subset of environments [5]. These data
63 indicate that, while understanding the factors driving individual element accumulation is
64 important, it is also necessary to consider the ionome as a network of co-regulated and
65 interacting traits [6]. Multivariate analysis techniques, such as principal components analysis
66 (PCA), reduce multivariate data dimension by minimizing the variances of multiple input factors
67 to new variables. When multiple phenotypes are correlated, such as for multiple elements in the
68 ionome, this approach may prove to be complementary to single element approaches so as to
69 better summarize these relationships.

70 Quantitative genetics using structured recombinant inbred populations is a powerful tool
71 for dissecting the factors underlying elemental accumulation and relationships. By breaking up
72 linkage blocks through recombination and then fixing these new haplotypes of diverse loci into
73 mosaic sets of lines, these populations allow similar sets of alleles to be repeatedly tested in
74 diverse environments [7]. A variety of quantitative statistical approaches can then be used to
75 identify QTL by environment interactions (QEI).

76 Here, we used elemental profiling of a maize recombinant inbred population grown in
77 multiple environments analyzed using both single and multivariate approaches to identify QTL
78 and QEI underlying elemental accumulation. By seeking both environmental and genetic
79 determinants, we detected loci controlling elemental accumulation, many of which were
80 environment-specific. We also show that multivariate approaches can reveal environmental and
81 genetic effects that cannot be detected using single element approaches.

82 Results

83 Genetic Regulation of Elemental Traits

84 The data used for this study is comprised of 20 elements measured in the seeds from *Zea*
85 *mays* L. Intermated B73 x Mo17 recombinant inbred line (IBM) populations grown in 10
86 different location/year settings. The IBM population is a widely studied maize population of 302
87 intermated recombinant inbred lines, each of which have been genotyped with a set of 4,217 bi-
88 allelic single nucleotide polymorphism (SNP) genetic markers [8]. The four rounds of
89 intermating and subsequent inbreeding resulted in more recombination and a longer genetic map
90 for the IBM than for typical biparental recombinant inbred line populations. The number of
91 individuals, marker density, and greater recombination facilitates more precise QTL localization
92 than a standard RIL population [9-14]. This greater resolution reduces the number of genes

93 within a QTL support interval and increases the utility of QTL mapping as a hypothesis test for
94 shared genetic regulation of multiple traits and aids in the discovery of the molecular identity of
95 genes affecting QTL. For this study, subsets of the IBM population were grown at Homestead,
96 Florida in 2005 (FL05) and 2006 (FL06), West Lafayette, Indiana in 2009 (IN09) and 2010
97 (IN10), Clayton, North Carolina in 2006 (NC06), Poplar Ridge, New York in 2005 (NY05),
98 2006 (NY06), and 2012 (NY12), Columbia, Missouri in 2006 (MO06), and Ukilima, South
99 Africa in 2010 (SA10) (Table S1). Single seeds were profiled for the quantities of 20 elements
100 using ICP-MS and these measurements were normalized to seed weight and technical sources of
101 variation using a linear model [15]. These normalized values are referred to as the elemental
102 traits.

103 Variation in the elemental traits was affected by both environment and genotype. All
104 elemental traits exhibited greater variation among genotype replicates grown across multiple
105 environments than among replicates within a single environment (Table 1). The broad-sense
106 heritability of seed weight, 15 of 21 elements in NY05, 13 of 21 elements in NC06, and and 13
107 of 21 elements in MO06 exceeded 0.60. Elements exhibiting low heritability within
108 environments corresponded to the elements that are prone to analytical artifacts or present near
109 the limits of detection by our methods, such as B, Al, and As. Seven elements had a broad sense
110 heritability of at least 0.45 in a single environment (NY05, NC06, and NY06) but less than 0.1
111 across all environments. This decrease in heritability across the experiment, which was
112 particularly striking for Mg, P, S, and Ni, is consistent with strong genotype by environment
113 interactions governing the accumulation of these elements.

114 **Table 1. Broad-sense heritability of element concentrations.**

Trait	All env	NY05	NC06	MO06

Seed Weight	0.51	0.59	0.69	0.89
B	0.02	0.35	0.51	0.06
Na	0.11	0.34	0.23	0.19
Mg	0.04	0.77	0.69	0.75
Al	0.10	0.39	0.50	0.08
P	0.04	0.62	0.69	0.33
S	0.05	0.73	0.77	0.51
K	0.07	0.69	0.72	0.36
Ca	0.15	0.65	0.63	0.77
Mn	0.16	0.80	0.80	0.75
Fe	0.07	0.76	0.73	0.63
Co	0.08	0.65	0.54	0.42
Ni	0.06	0.84	0.54	0.82
Cu	0.20	0.80	0.75	0.92
Zn	0.07	0.68	0.73	0.86
As	0.02	0.37	0.45	0.01
Se	0.04	0.32	0.35	0.68
Rb	0.03	0.49	0.45	0.69
Sr	0.07	0.61	0.48	0.53
Mo	0.29	0.85	0.73	0.96
Cd	0.55	0.71	0.69	0.24

NY05: 50 lines with 2 reps, 199 lines with 3 reps
NC06: 121 lines with 2 reps, 53 lines with 3 reps, 4 lines with 4 reps
MO06: 50 lines with 2 reps, 18 lines with 3 reps
*outliers for each element calculated with outlier removal function, designated as NA
*for each single environment, for each trait, only lines w/o missing data and with reps >1 used to calculate heritability

A stepwise algorithm, implemented via *stepwiseqtl* in the R package R/qtl [16], was used to map QTL for seed weight and 20 seed elemental phenotypes. The stepwise algorithm iterates through the genome and tests for significant allelic effects for each marker on a phenotype. Forward and backward regression was used to generate final genome-wide QTL models for each trait. This QTL mapping procedure was completed for each of the IBM populations from each of the 10 environments for all 21 traits as separate analyses. QTL significance were determined using a penalty score for adding QTL to the stepwise model derived by taking the 95th percentile of the highest LOD score achieved in 1000 runs of the *scanone* genome scan with random data [17].

The environmental dependence on QTL detection was first estimated by identifying QTL

132 common to multiple environments. If QTL detected in two or more growouts affected the same
133 element and localized less than 5 cM apart they were considered to be the same locus. A total of
134 79 QTL were identified for seed weight and the 20 elemental traits across these 10 environments
135 (Fig 1B &C). Of these, 63 were detected in a single environment and 16 QTL were detected in
136 multiple environments. The 16 QTL found in multiple environments included QTL detected in
137 nearly all of the environments and QTL detected in only two. One QTL for Mo accumulation, on
138 chromosome 1 in the genetic region containing the maize ortholog of the Arabidopsis
139 molybdenum transporter MOT1 [4], was found in nine environments (Fig 1A). Another QTL
140 affecting Cd accumulation, on chromosome 2 and without a clear candidate gene, was found in
141 eight environments. Other QTL were only present in a smaller set of environments, such as the
142 QTL for Ni accumulation on chromosome 9, which was found in five environments (Fig 1D).
143 The strength of association and percent variance explained showed strong differences between
144 environments even for these QTL that were detected in multiple environments (Table S2).

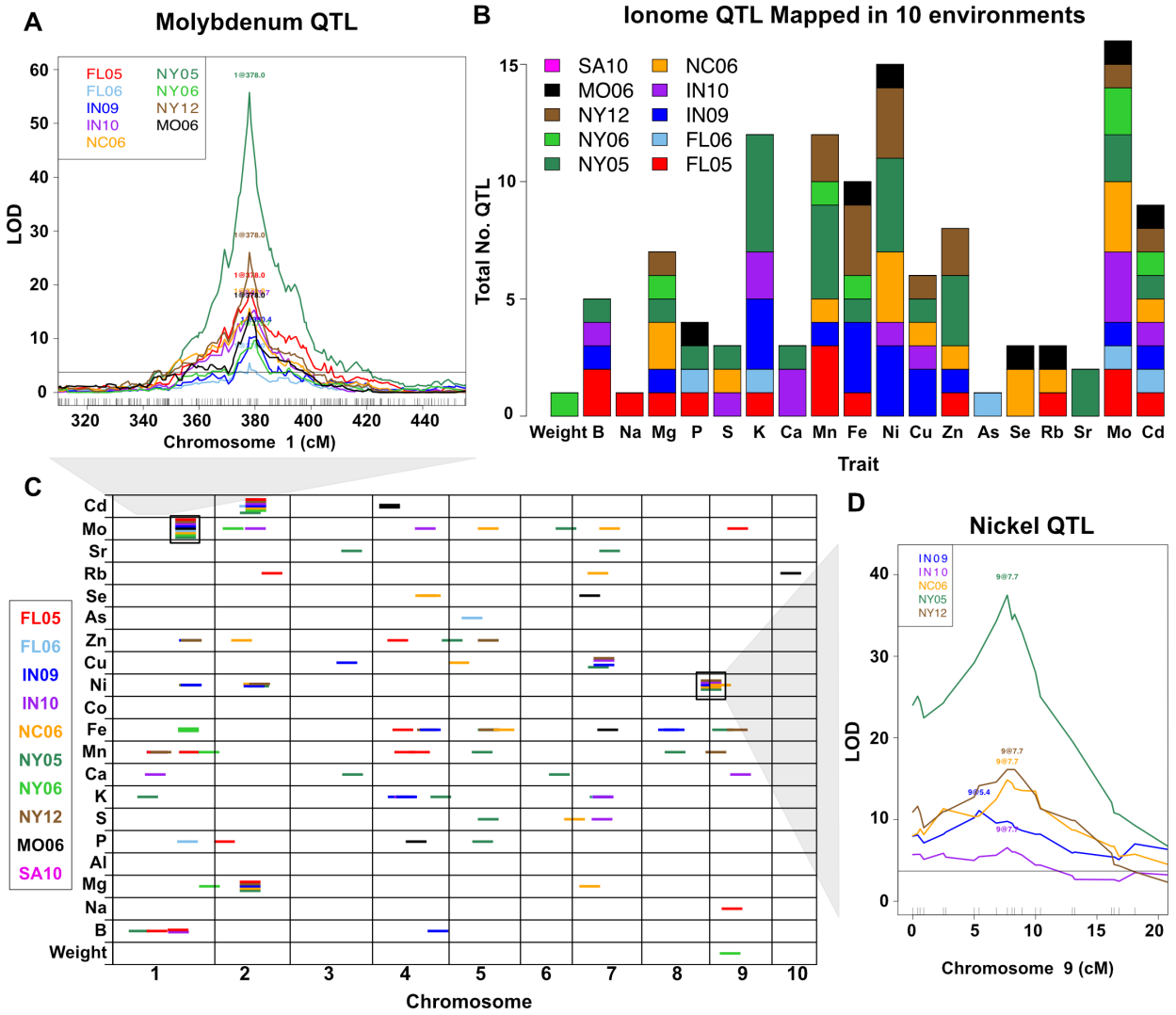

Fig 1. Ionome QTL from 10 Environments. QTL identified for seed weight and 20 element accumulation traits using the B73 x M017 intermated RIL population grown in 10 environments. (A) QTL on chromosome 1 affecting variation in molybdenum accumulation. An interval of Chr1 is shown on the x-axis (in centi-Morgans). The LOD score for the trait-genotype association is shown on the y-axis. The horizontal line is a significance threshold corresponding to the 95th percentile of highest LOD score from 1000 random permutations. The LOD profiles are plotted for all environments in which the highlighted QTL was detected. (B) Total number of QTL detected for each trait, colored by environment. (C) Significant QTL (loci with LOD scores at or above the 95th percentile of the highest LOD score achieved by running the stepwise QTL mapping algorithm on 1000 random permutation replicates) for each trait. QTL location is shown across the 10 maize chromosomes (in cM) on the x-axis. Dashes indicate QTL, with environment in which QTL was found designated by color. All dashes are the same length for visibility. The two black boxes around dashes correspond to LOD profiles traces in (A) and (D). (D) Stepwise QTL mapping output for nickel on chromosome 9. LOD profiles are plotted for all environments in which the QTL is significant.

161 As seen in the full-genome view of all QTL colored by environment (Fig 1C), there is a
162 high incidence of QTL found in single locations. There are three hypotheses that could explain
163 the large proportion of QTL found only in a single location: 1) strong QTL by environment
164 interaction effects, 2) false positive detection of a QTL in an individual location and 3) false
165 negatives assessment of QTL absence due to genetic action but statistical assessment below the
166 permutation threshold in other locations. To reduce the risk of false positives in a single
167 environment's QTL set, the significance threshold was raised to the 99th percentile, where 31 of
168 the 63 location-specific QTL remained significant. Using a Bonferroni correction for 200 tests
169 (20 traits in 10 environments), 10 QTL (95th percentile threshold) and two QTL (99th percentile
170 threshold) should exceed this threshold. The presence of 63 and 31 QTL greatly exceeds these
171 null approximations. To account for false negatives, we scanned for QTL using a more
172 permissive 75th percentile cutoff. Of the 63 single-environment QTL, only nine had QTL in other
173 environments by this more permissive threshold. Thus, the majority of the 63 single-environment
174 QTL most likely result from environmentally contingent genetic effects on the ionome.

175 **Accounting for Element to Element Correlations**

176 Previous elemental correlation studies and mutant phenotype analyses indicate extensive
177 relationships between elements [4,6]. In this experiment, several elements were highly correlated
178 across the dataset and nine loci were found with QTL for two or more different elements (Table
179 2). Phosphorous exhibited the highest incidence of shared QTL with other elements, including
180 shared QTL with the cations K and Mg and the only shared QTL found between more than two
181 elements, between P, S, Fe, Mn, and Zn in NY05 (Fig 2). Shared QTL were also found between
182 elements with similar structure, charge, and/or type, such as Ca and Sr or Fe and Zn.

183 **Table 2. QTL affecting variation for Multiple Elements in the same environment.**

Environment	Chr	Pos (cM) †	El 1	El 2	El 3	El 4	El 5
NY05	1	400	Mn	Ni	---	---	---
NY05	3	323	Sr	Ca	---	---	---
NY05	5	201	Mn	Zn	P	S	Fe
NY06	1	532	Mn	Mg	---	---	---
IN09	4	306	Fe	K	---	---	---
IN10	2	213	Mo	Cd	---	---	---
NY12	5	203	Zn	Fe	---	---	---
FL05	1	230	B	Mn	---	---	---
FL05	4	159	Fe	Zn	---	---	---

†Average position

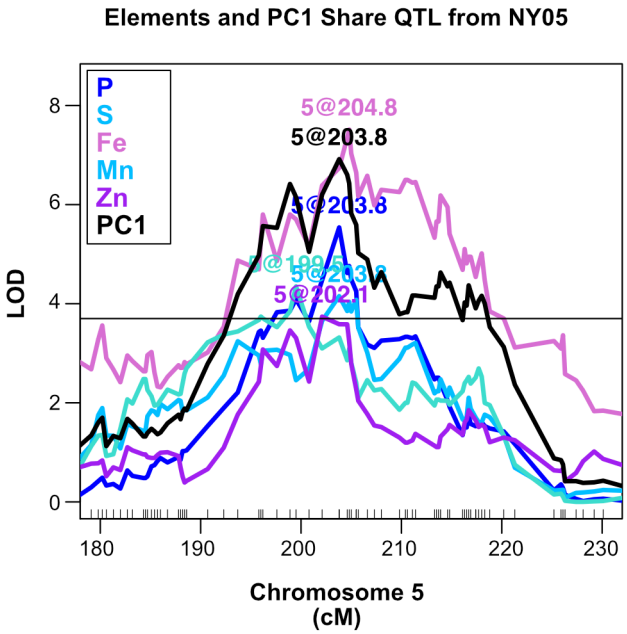

Fig 2. Multiple Element QTL. Stepwise QTL mapping output from the NY05 population for P, S, Fe, Mn, Zn, and PC1. Position in cM on chromosome 5 is plotted on the x-axis and LOD score is shown on the y-axis. 95th percentile of highest LOD score from 1000 random permutations is indicated as horizontal line.

To better identify factors underlying multi-element correlation, principal components analysis (PCA) was used. This reduced correlated elements into principal components (PCs), orthogonal variables that account for variation in the original dataset, each having an associated set of rotations from the input variables. PCA was conducted in each of the 10 environments separately. Elements that were difficult to measure and potentially introduce artifacts (B, Na, Al,

197 As) were excluded, as their covariance due to shared technical variation is problematic. The
198 remaining elemental data from lines within a single environment were transformed into 16
199 principal components (Fig S1). These 10 sets of 16 PCs were then used as traits for QTL
200 mapping.

201 QTL mapping using these derived traits yielded 101 QTL (Fig 3C). PC QTL overlapped
202 with many single element QTL, consistently recapitulating strong single element QTL seen for
203 elements such as Ni, Mo, and Cd. The PC QTL also capture previously observed multi-element
204 QTL. For example, in NY05, a QTL for PC1 overlaps the QTL that were detected in the single
205 element analyses of P, S, Fe, Mn, and Zn on chromosome 5 (Fig 2). The PC QTL in this case is
206 as strong as the Fe QTL and much more significant than the P, S, Mn, and Zn elemental QTL,
207 suggesting that a PC capturing multi-element variation may strengthen the signal acquired using
208 a single-element approach. In addition, mapping with PCs allowed for identification of new loci
209 not seen using single elements. QTL mapping on single elements may not have the power to
210 detect loci with small effects on several elements, so the unique QTL detected using PCs as traits
211 are of particular interest. For instance, two PC5 QTL from the NY06 growout on chromosome 1
212 were distinct from any elemental QTL (Fig 3B). 42 PC-specific QTL, defined as QTL >25 cM
213 away from any elemental QTL in the same environment, were detected. PCs are derived from
214 combinations of elements, and as a result single elemental QTL were reproduced for several PCs
215 within an environment. This is observed particularly for elements with strong single-element
216 effects, such as Mo and Cd. For example, in IN10, PC2 and PC10 have QTL that co-localize
217 with the same Cd QTL on chromosome 2. Likewise, in NY05, PC3, PC5, PC6, and PC9 all have
218 QTL that overlap with a single chromosome 9 Ni QTL. This redundancy contributes to the
219 higher number and proportion of detected PC QTL shared with element QTL (59/101) than

220 element QTL shared with PC QTL (28/79), although the same genomic locations underlie this

221 overlap (Fig 3A). The identification of unique QTL through this multivariate approach

222 demonstrates the complementary nature of working with trait covariance as well as the

223 component traits and shows that elemental traits are mechanistically interrelated [6,18].

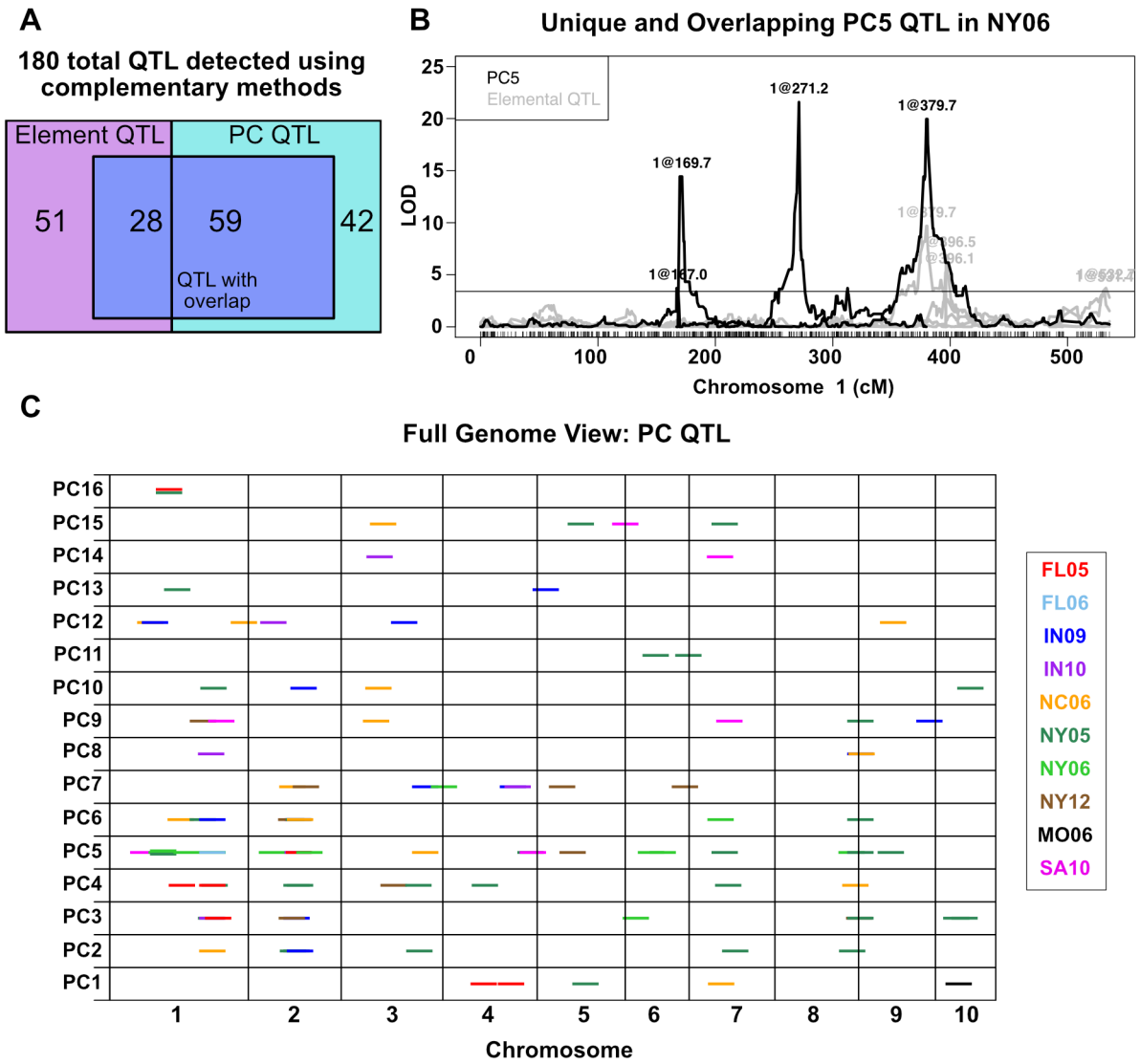

224

225 **Fig 3. Principal Component QTL from 10 environments.** PCs were derived from elemental
226 data from the IBM mapping population lines separately in each of 10 environments. 10 sets of 16
227 PCs, each set from a single environment, were used as traits for QTL mapping. (A) 180 total
228 element and PC QTL were mapped. The two boxes represent the 79 and 101 elemental and PC
229 QTL, respectively. 28 element QTL overlap with PC QTL from the same environment. 59 PC
230 QTL overlap with element QTL from the same environment. These sets of non-unique QTL are
231 shown in the box spanning both boxes. QTL unique to elements, 51, and to PCs, 42, are shown

outside of the shared box. (B) QTL mapping output for PC5 from the NY06 population. Chromosome 1 is shown on the x-axis (in cM), LOD score is on the y-axis. Significance threshold is calculated as 95th percentile of highest LOD score from 1000 random permutations. All significant NY06 element QTL on chromosome 1 are shown in grey. Two PC5 QTL, at 169.7 and 271.2 cM, are unique to PC5 and do not overlap with any elemental QTL. A PC5 QTL at 379.7 cM is shared with a molybdenum QTL. (C) Significant PC QTL (loci with LOD scores at or above the 95th percentile of the highest LOD score achieved by running the stepwise QTL mapping algorithm on 1000 random permutation replicates) for 16 PCs in 10 environments. QTL location is shown across the 10 maize chromosomes (in cM) on the x-axis. Environment in which QTL was found is designated by color. QTL are represented as dashes of uniform size.

QTL by Environment Interactions

That QTL detection was so strongly affected by environment suggested that the effects of allelic variation were heavily dependent on environments for both elemental and PCA traits. These results, however, did not specifically test for QTL by environment interactions (QEI). Comparison between environments in our data is additionally complicated because different subsamples of the IBM population were grown at these different locations and years. There are many different approaches to identifying QEI described in the literature, summarized in El-Soda et al. We took two previously implemented methods of QEI analysis. The first considered location (but not year) by comparing the goodness of fit for linear models with and without an interactive covariate [19-21]. The second method takes advantage of the ability to grow genetically identical RIL in multiple years. Trait values measured in the same IBM line for the same element at the same site but in different years were subtracted from each other and the difference between years was assigned as the trait value for that RIL genotype for QTL detection [22,23]. We added a third approach, not previously described, to determine the gene by environment effects on the multi-element phenotypes. We extended the PCA analysis across years and locations by calculating PCs on a subset of lines across environments, and using the loadings to calculate a projection for each line in each environment. If the genetic and environmental variances do not interact, some projections will reflect environmental variance

261 and others will reflect genetic variance. However, if the ionome is reporting on a summation of
262 physiological status that results from genetic and environmental influences, some projections
263 calculated from ionomic traits should be both correlated with environmental factors and result in
264 detectable QTL.

265 **Linear model estimation of QTL by location effects.** The most common approach to analyze
266 QEI is to fit a linear model with environment as both a cofactor and an interactive covariate and
267 compare results to a model with environment as an additive covariate [24]. This method is most
268 amenable when data are available for the same lines grown in every environment, which was not
269 the case across all of our dataset. Data from the three locations with two replicate years each (FL,
270 IN, NY) were analyzed to reduce the number of covariates and increase the power to detect
271 variation from the environment. The data for both years in each location were combined (FL05
272 & FL06, IN09 & IN10, NY05, NY06 & NY12), averaging common lines across years.

273 Two linear equations were fit to the combined data using the FL, IN, and NY locations as
274 covariates. The first equation is the full model considering phenotypic variation as controlled by
275 genotype and location as both additive and interacting covariates (1) while the reduced models
276 consider phenotypic variation as resulting from location and genotype as additive factors (2).
277 Subtracting (2) from (1) isolates genetic by location variation.

278 $$V_P = V_G + V_E + V_{GxE} \qquad (1)$$

279 $$V_P = V_G + V_E \qquad (2)$$

280 $$V_P = V_{GxE} \qquad (1) - (2)$$

281 The program R/qtl was used to fit QTL for phenotypic variation with and without
282 considering QTL by location interactions for sample weight and 20 elements. The significance
283 threshold was calculated by using the 95th percentile of the highest LOD score from 1000

284 permutations of the three step procedure (fitting the two models and then subtracting LOD
285 scores). Even with this underpowered dataset, 10 QTL by location interactions exceeded this
286 threshold (Table 3). Interactions between QTL and location are likely to be due to a combination
287 of soil and weather differences across different locations. In the case of Ni, our initial single-
288 element QTL mapping conducted separately on data from each environment identified
289 differences in QTL presence or strength between FL, IN, and NY locations (Fig 4). These QTL
290 corresponded to loci with significant QTL by location effect (Fig 4). Remarkably, all elemental
291 QTL by location interactions, detected by this approach, affected trace element accumulation.
292 These elements are both low in concentration in the grain, and often variable among soils [25].
293 Cd, an element for which we found significant QEI, has detrimental effects on both human and
294 plant health [26] and is toxic in food at levels as low as .05 ppm. [27]. The locus with the
295 strongest QEI for Cd does not follow location averages of Cd content in the grain (Table S3) and
296 therefore is unlikely to be affected by crossing a detection threshold driven by higher Cd in the
297 soils at those locations. This lack of direct correlation between QTL significance and grain
298 content also occurs for the loci with strong by-location effects for Mo and Ni. This demonstrates
299 that reduced cadmium or enhanced micronutrient contents in grain require plant breeding
300 selections that consider complex genetic by environment interactions rather than genotypes
301 assessed in a single soil environment.

302 **Table 3. QTL with Significant by-Location interactions.**

Trait	Chr	Pos (cM)	LOD	Significance Threshold†
Na	3	237.00	3.48	3.39
Na	9	115.40	4.24	3.39
Mn	1	232.00	4.77	3.84
Fe	5	196.20	3.69	3.57
Ni	9	7.70	23.59	5.44
Zn	4	157.40	3.82	3.78
Rb	2	188.40	4.30	3.41
Rb	10	93.60	4.25	3.41

Mo	1	378.00	32.85	4.32
Cd	2	214.60	14.47	3.59

303 †95th percentile LOD score from 1000 random permutations

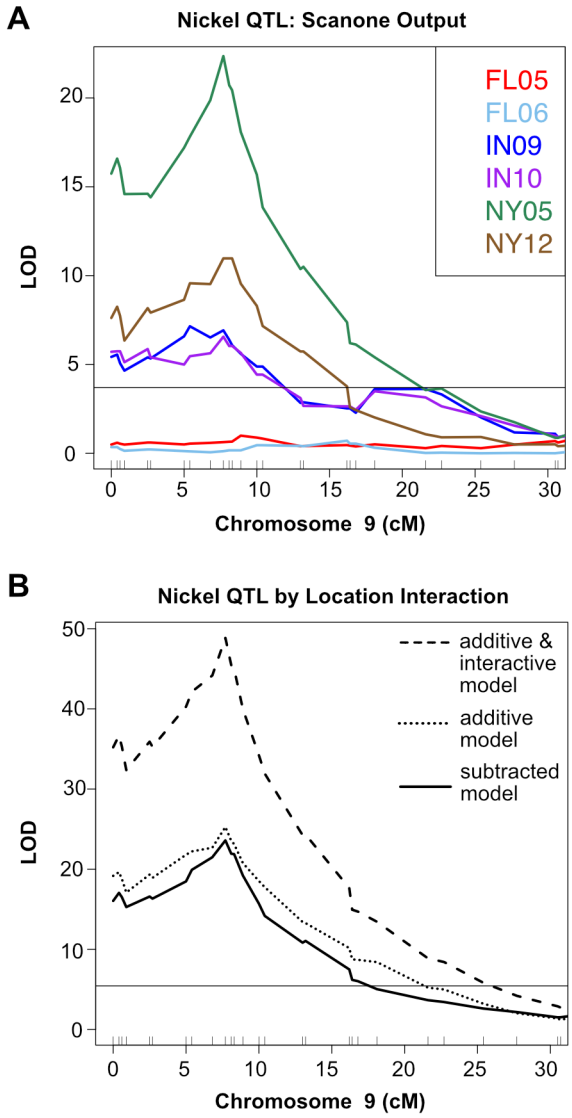

304

305 **Fig 4. Significant QTL-by-Location Interactions Reflect Variation in Single Environment**
306 **Mapping.** (A) Nickel QTL on chromosome 9 exhibits variation between FL, IN, and NY
307 growouts in single environment QTL mapping. Scanone QTL mapping output for Ni on is
308 plotted for FL05, FL06, IN09, IN10, NY05, and NY12. LOD score is plotted on the y-axis and
309 cM position on the x-axis. Horizontal line corresponds to 95th percentile of highest LOD score
310 from 1000 random permutations. (B) Scanone QTL mapping for combined Ni data from Florida
311 (FL05 and FL06), Indiana (IN09 and IN10), and New York (NY05 and NY12) growouts. All
312 lines within a location were included, with values averaged between lines common to multiple
313 years in a location. QTL mapping output using model with location as an additive covariate is
314 shown as dotted line. QTL mapping output from model with location as both an additive and
315 interactive covariate shown as dashed line. Subtracted LOD score profile from the two models

316 (QTL by location interactive effect only) shown as solid line. Horizontal line corresponds to
317 significance threshold for QTL by location interaction effect, derived from 1000 iterations of the
318 three step procedure using randomized data: scanone QTL mapping with the additive model,
319 scanone QTL mapping with the additive and interactive model, and subtraction of the two
320 models.
321
322 **QTL for trait differences within location.** The previous method identified genotypes with
323 interactions with location but not with year. Year to year variation will also have effects due to
324 differences in rainfall, temperature and management practices. To examine variation that occurs
325 within a location over different years, we examined the intra-location QEI in the three locations
326 (FL05 & FL06, IN09 & IN10, NY05 & NY12). Using the same stepwise algorithm that was
327 implemented with single element and PC analysis, QTL were mapped on the trait differences
328 between common lines in the two environments for sample weight and 20 elements. Mapping the
329 trait differences between years for the three locations identified loci affecting phenotypic
330 differences between the same lines grown on the same farm but in different years. Six QTL were
331 found for FL05-FL06 differences, one QTL for IN09-IN10 differences, and two QTL for NY05-
332 NY12 differences (Table 4). These trait-difference QTL included locations identified in our
333 single element and single environment QTL experiment where a locus was present for one year
334 but not the other or the QTL was found in both years with differing strength (Fig 5A, B, C). Six
335 QTL were detected that affected variation in the year to year difference but no QTL were
336 detected at that location when the years were mapped separately. This demonstrates that this
337 method can detect by-year differences that were not apparent by contrasting QTL detected from
338 each year's data. These significant effects of year to year environmental variation within the
339 same location indicated that factors beyond location are both influencing the ionome and
340 determining the consequences of genetic variation.
341 **Table 4. Significant QTL for Trait Differences.**

Location	Years Compared	Trait	Chr	Pos (cM)	LOD	Significance Threshold†
FL	FL05_FL06	Mg	8	294.4	5.23	3.74
FL	FL05_FL06	P	4	130.2	3.89	3.60
FL	FL05_FL06	P	4	297.8	6.03	3.60
FL	FL05_FL06	P	8	294.6	8.43	3.60
FL	FL05_FL06	Co	1	296.3	4.36	3.69
FL	FL05_FL06	Mo	1	378.6	6.10	3.70
IN	IN09_IN10	Fe	8	140.9	4.52	3.62
NY	NY05_NY12	K	5	154.2	4.25	3.61
NY	NY05_NY12	Sr	7	193.2	4.45	3.66

†95th percentile LOD score from 1000 random permutations

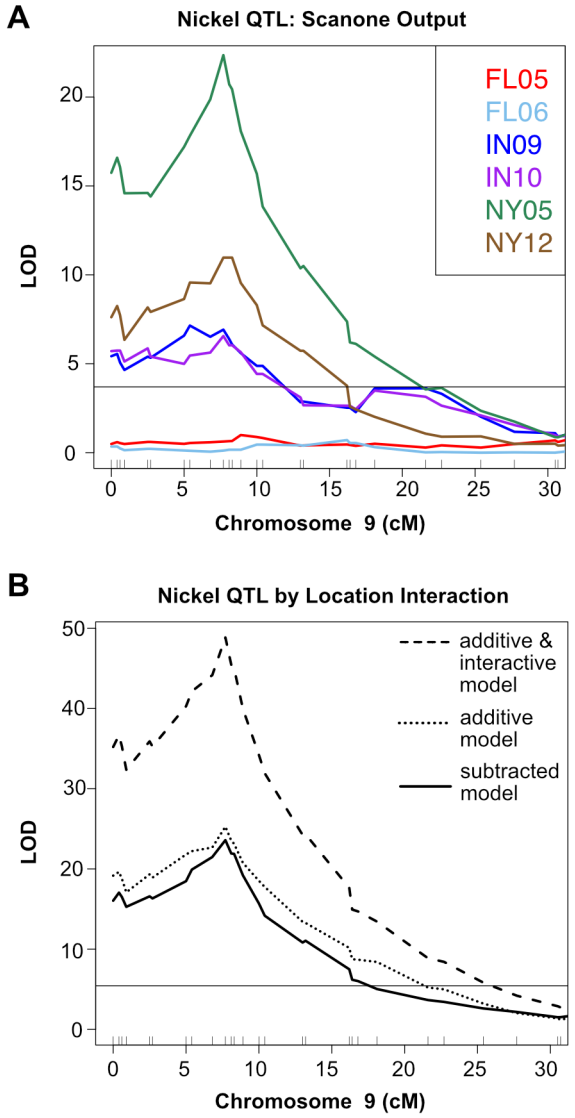

Fig 5. Comparison of QTL Mapped on Traits in Single Environments and Trait Differences Between Environments. Examples from stepwise QTL mapping on trait differences of between two years at one location, calculated between IBM lines common to both

347 years. Scanone QTL mapping output is plotted for the same trait from each year separately. LOD
348 score is plotted on the y-axis and cM position on the x-axis. Horizontal lines correspond to 95th
349 percentile of highest LOD score from 1000 random permutations. (A) Molybdenum QTL on
350 chromosome 1 mapped for Mo in FL05, Mo in FL06, and difference in Mo content between
351 FL05 and FL06. (B) Iron QTL on chromosome 8 mapped for Fe in IN09, Fe in IN10, and
352 difference in Fe content between IN09 and IN10. (C) Potassium QTL on chromosome 5 mapped
353 for K in NY05, K in NY12, and difference in K content between NY05 and NY12.
354
355 **PCA-derived projections.** The covariance between element accumulation data across all
356 environments was summarized using principal components analysis. Elements prone to
357 analytical artifacts (B, Na, Al, As) were removed prior to analysis. Only the 16 lines common to
358 six of the 10 environments (FL05, FL06, IN09, IN10, NY05, NY12) were used to calculate the
359 PCA. The rotations from this PCA were then projected onto the centered and scaled full dataset.
360 In this way, 16 projections (PRs) derived from PCs describing the covariation of the ionome
361 were calculated for every RIL in every environment. To reduce the incidence of artifacts or over
362 fitting, PRs accounting for less than 2% of the total variation were eliminated, leaving seven PRs
363 (Fig S2). The covariation captured by these PRs could due to genetic variation, result from a
364 programmed response of the plant across multiple environments, or a combination of both.
365 The first two PRs were highly responsive to the environment (Fig 6). The lines from each
366 environment cluster together when plotting PR1 vs PR2 values, with distinct separation between
367 environments and years. Additionally, when modeled as a simple linear function, environment
368 had a significant effect on all PRs ($p<0.001$). In order to identify environmental factors
369 responsible for ionome covariance, weather station data from each location and year was
370 collected from Climate Data Online (CDO) (http://www.ncdc.noaa.gov/cdo-web/). Average
371 minimum temperature, maximum temperature, and growing degree days (GDD = ((Tmax +
372 Tmin)/2) –10) across the entire 120-day growing season and over each 30-day quarter were
373 calculated from daily summaries (Fig. 7A). Correlations were calculated between weather

variables and average PR 1-7 values in the nine environments with weather data. Correlations were detected between PRs and weather variables. The weather variables, all temperature-based, are not correlated with PRs in many cases, although correlations exceeding r_p= 0.60 were observed for PRs 4-7 (Fig. 7A, Table S3). The strongest correlation observed for PR1 was with average maximum temperature in the fourth quarter of the growing season (r_p = 0.37) (Fig 7B) while the highest observed for PR2 was for average minimum temperature during the fourth quarter (r_p = 0.47) (Fig 7C). The relatively small number of environments, interrelatedness of the weather variables, and likely contribution of factors other than temperature limit the descriptive power of these correlations. The environmental components of projection variables are unknown but, consistent with element remobilization from the leaves to the seeds, temperature during the fourth quarter of the growing season may be one contributor to the environmental covariance in the seed ionome. The lack of particularly strong correlations between the first two PRs and temperature variables suggests that non-recorded variables, such as field to field variation in soil composition, fertilizer application, humidity, or biotic factors are likely to have an impact.

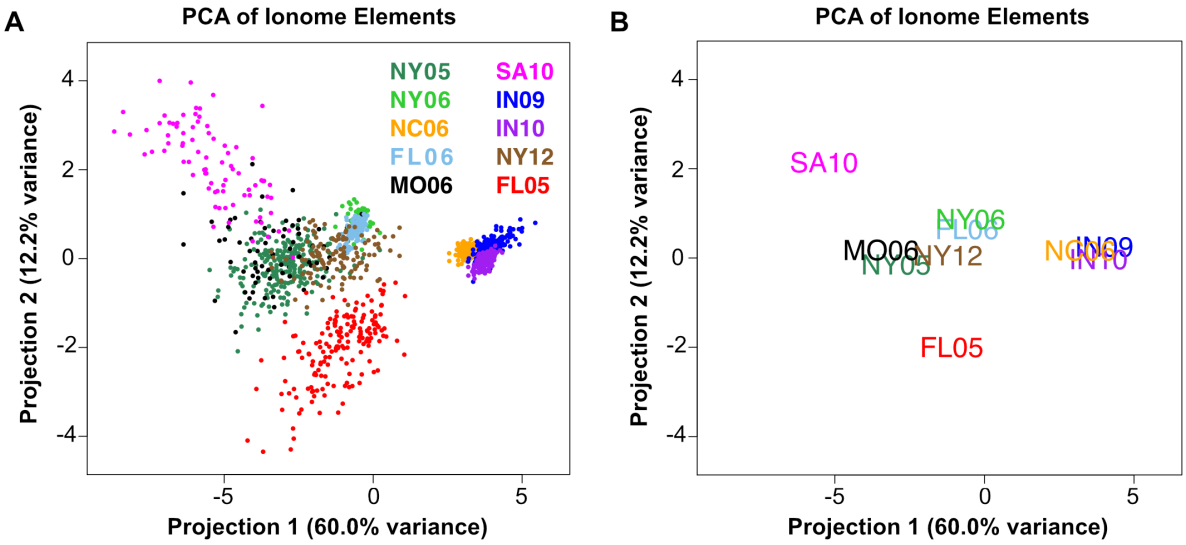

Fig 6. PC-Based Projections Separate Lines by Environment. PR1 and PR2 separate lines by environment. Points correspond to lines, colored by their environment. (A) PR1 vs PR2 values

for each line, colored by environment. Percentage of total variance accounted for by each PR indicated on the axes. (B) Average PR1 vs PR2 values for all lines in each environment.

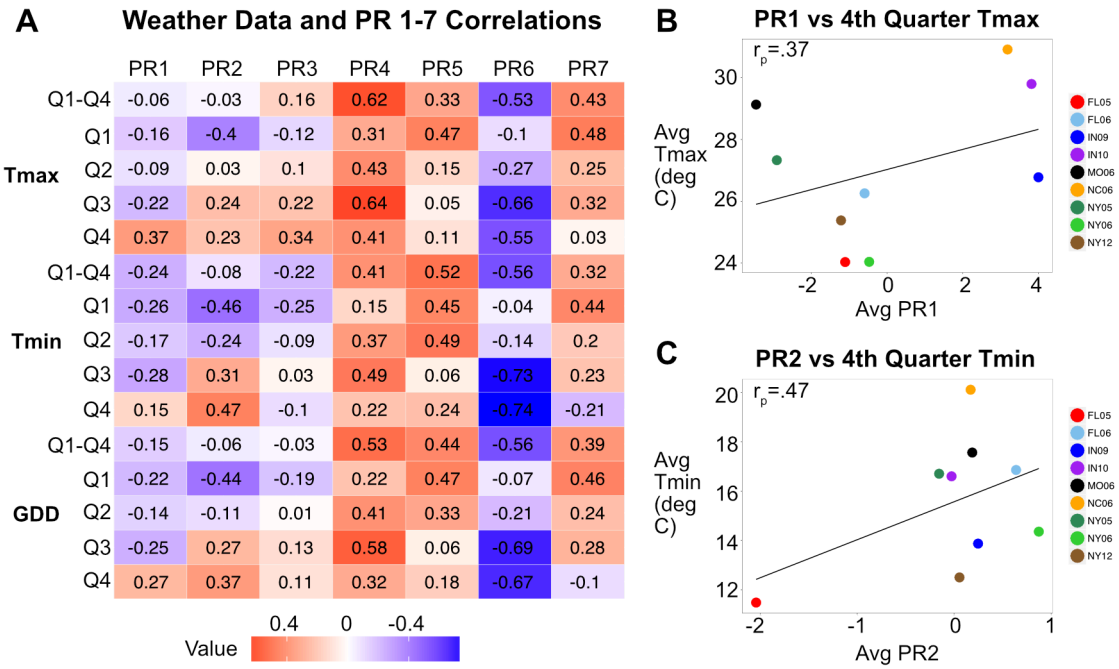

Fig 7. PR and Weather Variable Correlations. (A) Heatmap showing correlations between averaged PR 1-7 values across environments and averages for maximum temperature, minimum temperature, and growing degree days (GDD = (Tmax + Tmin)/2 –10)) across the entire growth season and for each quarter of the growth season. Red intensity corresponds to size of positive correlations. Blue intensity corresponds to magnitude of negative correlations. (B) Averaged PR1 values for 9 environments (FL05, FL06, IN09, IN10, NC06, NY05, NY06, NY12, MO06) plotted on x-axis. Average maximum temperature (in degrees Celsius) for each environment over the fourth quarter of the growing season plotted on the y-axis. Points are colored by environment. Pearson correlation coefficient (r_p = .37) is shown above the graph. (C) Averaged PR2 values for 9 environments plotted on x-axis. Average minimum temperature (in degrees Celsius) for each environment over the fourth quarter of the growing season plotted on the y-axis. Points are colored by environment. Pearson correlation coefficient (r_p = .47) is shown above the graph.

In order to determine genetic effects on these projections, the calculated values for PR1 through PR7 were used as traits for QTL analysis in each of the 10 environments. Unlike the earlier described PCAs done in environments separately, these PRs are calculated on data from all environments at once. Thus, while the single-environment PCs are distinct between environments, i.e. PC1 in NY05 does not have the same loadings as PC1 in NY06, the PRs are derived from PCs that account for across-environment variance and as such are the same trait for

415 mapping in each environment. The mapping analysis yielded at least four QTL for each PR and a
416 total of 44 QTL, eight of which were found in multiple environments and 36 in single
417 environments (Fig 8). Of these multi-environment QTL, 3 are overlapped with the three
418 strongest single element QTL (Mo on Chr1, Cd on Chr 2 and Ni on Chr 9). The Mo and Cd QTL
419 overlap with QTL from different PRs (PRs 3-6 for Mo and PRs 1-5 for Cd) depending on
420 environment while the Ni QTL is only present in PR6 in the NY environments. The presence of
421 PR QTL demonstrate that the covariation in the ionome described by PRs 1-7 results from both
422 environmental and genetic variation. Further investigation is needed to identify the genes
423 underlying PR QTL, their biological roles, and their interaction with specific environmental
424 variables.

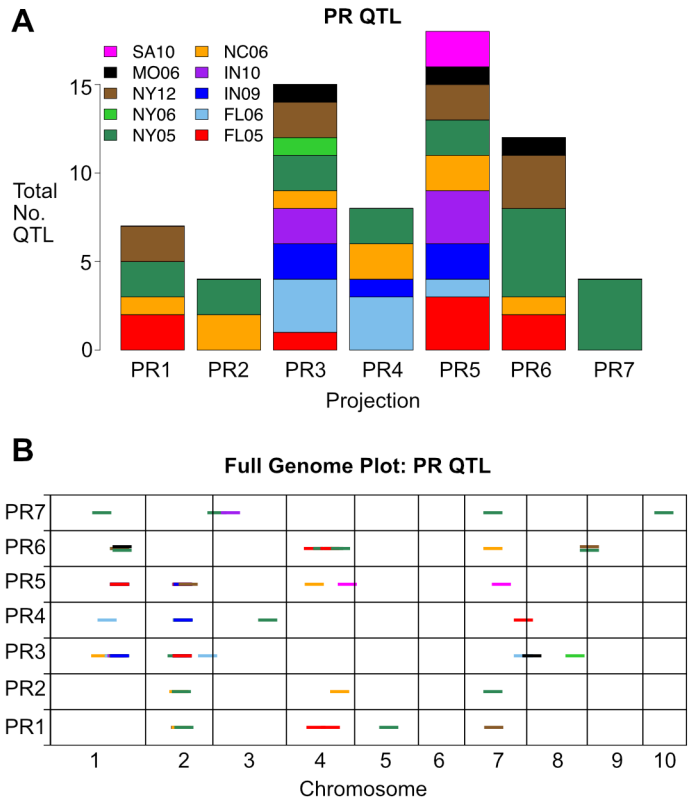

425

426 **Fig 8. PR QTL in 10 Environments.** QTL identified for PCA-derived projection traits (PRs 1-
427 7). (A) Total number of QTL detected for each PR, colored by environment. (B) Significant
428 QTL (loci with LOD scores at or above the 95th percentile of the highest LOD score achieved by

429 running the stepwise QTL mapping algorithm on 1000 random permutation replicates) for PRs
430 1-7. QTL location is shown across the 10 maize chromosomes (in cM) on the x-axis. Dashes
431 indicate QTL, with environment in which QTL was found designated by color. All dashes are the
432 same length for visibility.

433 Discussion

434 The results described here demonstrate that the concentrations of elements in the kernels
435 of maize are highly interrelated. Dramatically, and perhaps paradoxically, element concentration
436 is highly heritable within an environment and varied between environments. In agreement with
437 previous studies, we found elemental correlations and QTL that were detected for more than one
438 element. Phosphorous exhibited the greatest number of QTL overlap with other elements,
439 including the cations K and Mg. Phosphorous is a central nutrient in plant development and
440 regulates other elements. In the form of phytate, phosphorous complexes with cations to form
441 phytin in maize seeds [28]. Additional shared QTL included those between Ca and Sr, Mo and
442 Mn, and Zn and Fe. Ca and Sr are chemical analogs while Zn and Fe regulation have been linked
443 at the physiological and molecular level [4,29]. Mo and Mn have roles in protein assimilation
444 and nitrate regulation [30,31] and exhibit a regulatory relationship [18]. Thus, these shared QTL
445 likely reflect the coincident genetic regulation of multiple elements and demonstrate cellular
446 mechanisms to detect and respond to the levels of those elements.

447 Given the importance of understanding the effects of genetic alteration of multi-element
448 regulatory genes or genetic changes targeted to a single element with pleiotropic effects on other
449 elements, multivariate methods are necessary to create a fuller understanding of the factors
450 underlying ionomic variation. PCA generated variables representative of multiple elements and
451 condensed the covariation between elements without requiring that we know of specify the
452 underlying relationships that led to covariance. QTL mapping with the principal components as
453 traits isolated both loci that had been identified using elements as traits and PC-specific QTL.

454 The PC-specific QTL likely represent loci with small effects on multiple elements which would
455 not be detected when considering only the concentration of single elements. Candidate genes for
456 these QTL include transporters with multi element specificities or factors within a pathways
457 responding to several elements. Clearly, the inability to detect multiple element loci would leave
458 substantial gaps in our understanding of element regulatory networks, making PCA a useful
459 complement to single element approaches.

460 The presence of a large number of single-environment QTL is consistent with the
461 hypothesis that environment has a significant impact on genetic factors influencing the ionome.
462 By changing the stringency of the statistical tests, we are able to discount the likelihood that that
463 these single environment QTL are the result of a large number of false positives or false
464 negatives. The structure of our data, with few lines measured across all locations and years,
465 limited our ability to test for direct QTL by Environment Interactions. As a result, we have likely
466 underestimated the extent of QEI. Future studies with uniform lines across environments will
467 allow for inclusion of data from all environments and lines and increase power to detect
468 additional genetic by environment interactions.

469 Nevertheless, we were able identify QEI over different locations and QEI at a single
470 location over different years. We identified a strong nickel QTL on chromosome 9 that was
471 found in Indiana and New York with single-environment QTL mapping, but not in Florida. This
472 same locus also identified as a significant location-interacting QTL when using a model that
473 included Indiana, New York, and Florida as covariates. One possible cause for this, and other
474 location specific QTL, might be differences in element availability between local soil
475 environments. Interestingly, the presence/absence of the QTL does not seem to correlate with the
476 mean levels of the elements in the grains sampled from that location, suggesting that QEI are not

477 being driven solely by altered availability of the elements in the soil. Local soil differences are
478 less likely to be driving the QTL found for pairwise differences between two years at one
479 location. Soil content should remain relatively similar from year to year at the same farm,
480 suggesting that the loci identified by comparison between years and within location will encode
481 components of elemental regulatory processes responsive to precipitation, temperature, or other
482 weather changes.

483 In addition to being a tool for understanding the genetics of multi-element regulation,
484 principal components were also used as a tool to reflect environmental variation in the ionome
485 and genetic by environment interactions. Rather than simply conduct a PCA on all lines, the two-
486 step procedure of generating projections from a PCA on lines replicated within a subset of
487 environments was used to find variables that could describe variation across all 10 environments
488 while minimizing the confounding effect of different sets of lines among all environments. The
489 first two projections capture most of the variation in the ionome across 10 different growouts,
490 much of which is environmental. This can be seen in the ability of PR1 and PR2 to separate
491 growouts by location and, in some cases, different years within a location. Thus, PRs capture the
492 impact of environment on the ionome as a whole. Within the data collected, limited to only
493 maximum and minimum temperature, we observed the strongest correlations for PR1 and PR2
494 during the fourth quarter of the growing season. Because seed filling occurs in the last quarter of
495 the season, temperature during this time could have a pronounced affect on seed elemental
496 composition. However, given the presence of a low number of data points and a lack of any
497 striking correlations, environmental components of the projections must be largely explained by
498 environmental factors other than temperature. Experiments with more extensive weather and soil
499 data, or carefully manipulated environmental contrasts, are needed to create models with

500 additional covariates and precisely model environmental impacts. The identification of PR QTL
501 indicated that the variation captured by PRs has both environmental and genetic components.
502 These QTL may encompass genes that affect the ionome in an environmentally-responsive
503 manner.

504 Although the mapping intervals do not provide gene-level resolution, several QTL
505 overlap with known elemental regulation genes, such as the QTL on chromosome 1 at 378 cM
506 which coincides with ZEAMMB73_045160, an ortholog of the Arabidopsis molybdenum
507 transporter, MOT1. We observe strong effects and replication of this QTL across nearly all
508 environments, suggesting that this MOT1 plays a role in a variety of environments. Other large
509 effect QTL found in several environments merit further investigation, as they may recapitulate
510 important element-associated genes that have yet to be identified. Identification of the genes
511 underlying these QTL and the gene/environmental variable pairs underlying the QEIs will
512 improve our understanding of the factors controlling plant elemental uptake and productivity.
513 Given the high levels of variability that the interaction between genotype and environmental
514 factors can induce in these traits, conventional breeding approaches that look for common
515 responses across many different environments for a single trait may fail to improve the overall
516 elemental content, necessitating rational approaches that include both genetic and environmental
517 factors.

518 **Conclusions**

519 Here we have shown that the maize kernel ionome is determined by genetic and
520 environmental factors, with a large number of genetic by environment interactions. Elemental
521 profiling of the IBM population across 10 environments allowed us to capture environmentally-
522 driven variation in the ionome. Our QTL analysis on single elements found mainly single-

523 environment QTL, indicative of substantial genetic by environment interaction in establishment
524 of the elemental composition of the maize grain. We also demonstrated that treating the ionome
525 as an interrelated set of traits using PCA within environments can identify novel loci. PCA
526 across environments allowed us to derive projections that described both environmental and
527 genetic variation in the ionome. This approach, along with identification of QEI occurring both
528 within a single location over different years and QEI between different locations, demonstrated
529 that gene by environment interactions underlie elemental accumulation in maize kernels.

530 # Methods

531 **Field Growth and Data Collection**

532 **Population and field growth.** Subsets of the intermated B73 x Mo17 recombinant inbred (IBM)
533 population were grown in 10 different environments: Homestead, Florida in 2005 (220 lines)
534 and 2006 (118 lines), West Lafayette, Indiana in 2009 (193 lines) and 2010 (168 lines), Clayton,
535 North Carolina in 2006 (197 lines), Poplar Ridge, New York in 2005 (256 lines), 2006 (82 lines),
536 and 2012 (168 lines), Columbia, Missouri in 2006 (97 lines), and Ukilima, South Africa in 2010
537 (87 lines). In all but three environments, NY05, NC06, and MO06, one replicate was sampled
538 per line. In NY05, 3 replicates of 199 lines, 2 replicates of 50 lines, and 1 replicate of 7 lines
539 were sampled. Table S1 includes planting dates and line numbers after outlier removal and
540 genotype matching.

541 **Elemental Profile Analysis**

542 Elemental profile analysis is conducted as a standardized pipeline in the Baxter Lab. The
543 methods used for elemental profile analysis are as described in Ziegler et al. Descriptions taken
544 directly are denoted by quotation marks.

545 **Sample preparation and digestion.** Lines from the IBM population from each environment
546 were analyzed for the concentrations of 20 elements. "Seeds were sorted into 48-well tissue
547 culture plates, one seed per well. A weight for each individual seed was determined using a
548 custom built weighing robot. The weighing robot holds six 48-well plates and maneuvers each
549 well of the plates over a hole which opens onto a 3-place balance. After recording the weight,
550 each seed was deposited using pressurized air into a 16×110 mm borosilicate glass test tube for
551 digestion. The weighing robot can automatically weigh 288 seeds in approximately 1.5 hours
552 with little user intervention."
553 "Seeds were digested in 2.5 mL concentrated nitric acid (AR Select Grade, VWR) with
554 internal standard added (20 ppb In, BDH Aristar Plus). Seeds were soaked at room temperature
555 overnight, then heated to 105°C for two hours. After cooling, the samples were diluted to 10 mL
556 using ultrapure 18.2 MΩ water (UPW) from a Milli-Q system (Millipore). Samples were stirred
557 with a custom-built stirring rod assembly, which uses plastic stirring rods to stir 60 test tubes at a
558 time. Between uses, the stirring rod assembly was soaked in a 10% HNO_3 solution. A second
559 dilution of 0.9 mL of the 1st dilution and 4.1 mL UPW was prepared in a second set of test tubes.
560 After stirring, 1.2 mL of the second dilution was loaded into 96 well autosampler trays."
561 **Ion Coupled plasma mass spectrometry analysis.** Elemental concentrations of B, Na, Mg, Al,
562 P, S, K, Ca, Mn, Fe, Co, Ni, Cu, Zn, As, Se, Rb, Sr, Mo, and Cd "were measured using an Elan
563 6000 DRC-e mass spectrometer (Perkin-Elmer SCIEX) connected to a PFA microflow nebulizer
564 (Elemental Scientific) and Apex HF desolvator (Elemental Scientific). Samples were introduced
565 using a SC-FAST sample introduction system and SC4-DX autosampler (Elemental Scientific)
566 that holds six 96-well trays (576 samples). All elements were measured with DRC collision
567 mode off. Before each run, the lens voltage and nebulizer gas flow rate of the ICP-MS were

568 optimized for maximum Indium signal intensity (>25,000 counts per second) while also
569 maintaining low CeO+/Ce+ (<0.008) and Ba++/Ba+ (<0.1) ratios. This ensures a strong signal
570 while also reducing the interferences caused by polyatomic and double-charged species. Before
571 each run a calibration curve was obtained by analyzing six dilutions of a multi-element stock
572 solution made from a mixture of single-element stock standards (Ultra Scientific). In addition, to
573 correct for machine drift both during a single run and between runs, a control solution was run
574 every tenth sample. The control solution is a bulk mixture of the remaining sample from the
575 second dilution. Using bulked samples ensured that our controls were perfectly matrix matched
576 and contained the same elemental concentrations as our samples, so that any drift due to the
577 sample matrix would be reflected in drift in our controls. The same control mixture was used for
578 every ICP-MS run in the project so that run-to-run variation could be corrected. A run of 576
579 samples took approximately 33 hours with no user intervention. The time required for cleaning
580 of the instrument and sample tubes as well as the digestions and transfers necessary to set up the
581 run limit the throughput to three 576 sample runs per week."

582 **Computational Analysis**

583 **Drift correction and analytical outlier removal.** Analytical outliers were removed from single-
584 seed measurements using a method described in Davies and Gather (1993). Briefly, values were
585 considered an outlier and removed from further analysis if the median absolute deviation
586 (MAD), calculated based on the line and location where the seed was grown, was greater than
587 6.2.

588 Normalization for seed weight by simply dividing each seed's solution concentration by
589 sample weight resulted in a bias where smaller seeds often exhibited a higher apparent elemental
590 concentration, especially for elements whose concentration is at or near the method detection

591 limit. This bias is likely either a result of contamination during sample processing, a systematic
592 over or under reporting of elemental concentrations by the ICP-MS or a violation of the
593 underlying assumption that elemental concentration in seeds scales linearly with seed weight.
594 Instead, we developed a method whereby the residuals from the following linear model:
595

596 $$Y = \beta_0 + \beta_1 X_1 + \beta_2 X_2 + e$$

597

598 where Y is the non-weight normalized measure of elemental concentration for each seed after
599 digestion, β_0 is the population mean, X_1 is the seed weight, X_2 is the analytical experiment the
600 seed was run in (to further correct for run-to-run variation between analytical experiments), and e
601 is the residual (error) term. The residuals in this linear model represent how far each data point
602 departs from our assumption that analyte concentration will scale linearly with sample weight. If
603 all samples have the same analyte concentration then the linear model will be able to perfectly
604 predict analyte concentration from weight and the residuals will all equal zero. However, if a
605 sample has a higher or lower concentration of an analyte then the general population being
606 measured, then it will have a residual whose value represents the estimated concentration
607 difference from the population mean. For this reason, we have termed this value the estimated
608 concentration difference from the mean (ECDM).
609 **Heritability calculation.** Broad-sense heritability was calculated for seed weight and 20
610 elements across environments and within three environments for which we had substantial
611 replicate data. To calculate the broad-sense heritability across 10 environments, the total
612 phenotypic variance was partitioned into genetic and environmental variance, with the broad-
613 sense heritability being the fraction of phenotypic variance that is genetic. This was done using

614 an unbalanced, type II analysis of variance (ANOVA) in order to account for the unbalanced
615 common line combinations across environments. Two models were fit using the *lmfit* function in
616 R. The first model included genetic variance as the first term and environmental variance as the
617 second. The second model had the opposite form. The sum of squares for genetic or
618 environmental components was obtained using the *anova* function on the model in which that
619 component was the second term. Broad-sense heritability was calculated by dividing the genetic
620 sum of squares by the total (genetic plus environmental) sum of squares. Heritability was
621 calculated within environments for NY05, NC06, and MO06. Data with outliers designated as
622 NA was used for each environment. For each element within an environment, lines with NA
623 were removed and lines with only 1 replicate were removed, leaving only lines with 2 or more
624 replicates. The heritability was then calculated for seed weight and each element using *lmfit*
625 followed by *anova* functions to obtain the sum of squares for the genetic component and the
626 residuals. Broad-sense heritability was calculated as the proportion of total variance (genetic plus
627 residuals) explained by the genetic component.
628 **QTL mapping: elemental traits.** The R package R/qtl was used for QTL mapping. For each of
629 the 10 environments, elemental trait line averages and genotypes for all lines, 4,217 biallelic
630 single nucleotide polymorphisms (SNPs) distributed across all 10 maize chromosomes, were
631 formatted into an R/qtl cross object. The *stepwiseqtl* function was used to implement the
632 stepwise method of QTL model selection for 21 phenotypes (seed weight, 20 elements). The max
633 number of QTL allowed for each trait was set at 10 and the penalty for addition of QTL was set
634 as the 95th percentile LOD score from 1000 *scanone* permutations, with imputation as the
635 selected model for *scanone*. A solely additive model was used; epistatic and interaction effects
636 were not considered and thus heavy and light interaction penalties were set at 0. QTL positions

637 were optimized using *refineqtl*, which considers each QTL one at a time, in random order,
638 iteratively scanning in order to move the QTL to the highest likelihood position. QTL models for
639 each trait in each environment were obtained using this procedure. QTL within 5 cM of each
640 other were designated as the same QTL.

641 **Principal components analysis.** Elements prone to analytical error were removed prior to PC
642 analysis, leaving 16 elements (Mg, P, S, K, Ca, Mn, Fe, Co, Ni, Cu, Zn, Se, Rb, Sr, Mo, and Cd)
643 that were used for PCA. A PCA was done using elemental data for each of the 10 environments
644 separately. The *prcomp* function in R with scale = TRUE was used for PCA on elemental data to
645 perform PCA on the line average element values in an environment. This function performs
646 singular value decomposition on a scaled and centered version of the input data matrix,
647 computing variances with the divisor *N*-1. 16 PCs were returned from each environment and the
648 10 sets of 16 PCs were used as traits in QTL analysis.

649 **QTL Mapping: principal components.** QTL mapping was done in the same manner as
650 described for element phenotypes but with principal components as phenotypes. The mapping
651 procedure was done for each environment separately, with PC line averages for each line in the
652 given environment as phenotypes and line genotypes as input. The stepwise algorithm was used
653 with the same designations as with single-element mapping to produce a QTL model for each PC
654 The PC QTL were compared to element QTL, with unique PC QTL designated as PC QTL at
655 least 25 cM away from any element QTL detected in the environment in which the PC QTL was
656 detected.

657 **QTL by environment analysis: linear model comparison.** Linear modeling was used
658 determine instances and strength of QEI using data averaged over years within a three locations
659 (FL, IN, NY). FL05 and FL06 data were combined, averaging for common lines. The same was

660 done with IN09 and IN10 and with NY05, NY06 and NY12. FL, IN, and NY were then used as
661 covariates in QTL analysis. Two QTL models were fit for each phenotype (sample weight, 20
662 elements, 7 PCs) using the *scanone* function in R/qtl: (1) a model of phenotypic variation with
663 location as an additive and interacting covariate and (2) a model of phenotypic variation with
664 location as only an additive covariate. LOD scores for each marker using model (2) were
665 subtracted from LOD scores for each marker using model (1) to isolate genetic by location
666 variation.

667 $$V_P = V_G + V_E + V_{GxE} \qquad (1)$$

668 $$V_P = V_G + V_E \qquad (2)$$

669 $$V_P = V_{GxE} \qquad (1) - (2)$$

670 QTL by location interaction was determined as QTL with a significant LOD score after
671 subtraction. The significance threshold was calculated from 1000 permutations of the three step
672 procedure (fitting the two models and then subtracting LOD scores) and taking the 95th
673 percentile of the highest LOD score.

674 **QTL by environment analysis: mapping on within-location differences.** QTL were mapped
675 on phenotypic differences between common lines grown over two years at a single location. This
676 procedure was used to compare FL05 and FL06, IN09 and IN10, and NY05 and NY12 by
677 calculating the differences for each trait value between common lines in location pairs (FL05-
678 FL06, IN09-IN10, NY05-NY12) and using these differences for analysis using the previously
679 described *stepwiseqtl* mapping and permutation procedure.

680 **QTL by environment analysis: PCA-derived projections.** The 16 most precisely measured
681 elements (Mg, P, S, K, Ca, Mn, Fe, Co, Ni, Cu, Zn, Se, Rb, Sr, Mo, and Cd) were used for
682 principal components analysis. The *prcomp* function in R with scale = TRUE was used for PCA

683 on elemental data to perform PCA on only the 16 lines common to 6 of the 10 environments in
684 which we had two replicates per location (FL05, FL06, IN09, IN10, NY05, NY12). PC loadings
685 were extracted from the *prcomp* object and then matrix multiplied with the centered and scaled
686 full dataset matrix (all lines, all environments) to generate whole dataset projections (PRs) of
687 PCs influenced by only lines with multi-environment replicates. The first 7 PRs, derived from
688 the first 7 PCs (98% total variation), were used for correlation analysis with weather variables
689 and stepwise QTL mapping.
690 **Weather data collection and analysis.** Weather data for FL05, FL06, IN09, IN10, NC06,
691 NY05, NY06, and NY12 was collected from Climate Data Online (CDO), an archive provided
692 by the National Climatic Data Center (NCDC) through the National Oceanic and Atmospheric
693 Administration website: http://www.ncdc.noaa.gov/cdo-web/. The Climate Data Online Search
694 was used to find Daily Summaries for each day of the growing season from the weather station
695 nearest to the field location. For Florida growouts (FL05, FL06), data was collected from the
696 Homestead General Aviation Airport station. For Indiana growouts (IN09, IN10): West
697 Lafayette 6 NW station. North Carolina (NC06): Clayton station. New York growouts (NY05,
698 NY06, NY12): Aurora Research Farm station. Missouri (MO06): Columbia U of M station.
699 Minimum temperature (in degrees Celsius), and maximum temperature (in degrees Celsius) was
700 available in each location. With these variables, average minimum temperature, and maximum
701 temperature were calculated across the 120-day growing season as well as for 30 day quarters.
702 GDD was calculated for the entire season and quarterly using the formula GDD = ((Tmax +
703 Tmin)/2) –10. Weather data averages for all environments except for South Africa were tested
704 for correlation with the PR averages from the corresponding 9 environments. The pearson
705 correlation coefficient was calculated for pairs between weather variables and PRs 1-7.

Acknowledgements

The authors would like to thank Justin Borevitz and Riyan Cheng, and Tom Juenger for advice on QTL by environment mapping, Karl Broman for invaluable assistance with R/qtl and Sherry Flint-Garcia, Peter Balint-Kurti and Torbert Rocheford for providing seed.

References

1. McDowell SC, Akmakjian G, Sladek C, Mendoza-Cozatl D, Morrissey JB et al. (2013) Elemental Concentrations in the Seed of Mutants and Natural Variants of *Arabidopsis thaliana* Grown under Varying Soil Conditions. PLoS ONE 8: e63014.
2. Cobb JN, DeClerck G, Greenberg A, Clark R, McCouch S (2013) Next-generation phenotyping: requirements and strategies for enhancing our understanding of genotype-phenotype relationships and its relevance to crop improvement. Theor Appl Genet 126: 867-887.
3. Lahner B, Gong J, Mahmoudian M, Smith EL, Abid KB et al. (2003) Genomic scale profiling of nutrient and trace elements in Arabidopsis thaliana. Nat Biotechnol 21: 1215-1221.
4. Baxter I, Muthukumar B, Park HC, Buchner P, Lahner B et al. (2008) Variation in Molybdenum Content Across Broadly Distributed Populations of *Arabidopsis thaliana* Is Controlled by a Mitochondrial Molybdenum Transporter (*MOT1*). PLoS Genet 4: e1000004.
5. Buescher E, Achberger T, Amusan I, Giannini A, Ochsenfeld C et al. (2010) Natural genetic variation in selected populations of Arabidopsis thaliana is associated with ionomic differences. PLoS One 5: e11081.
6. Baxter I (2009) Ionomics: studying the social network of mineral nutrients. Current

729 Opinion in Plant Biology 12: 381-386.
730 7. Koornneef M, Alonso-Blanco C, Peeters AJM (1997) Genetic approaches in plant
731 physiology. New Phytologist 137: 1-8.
732 8. Lee M, Sharopova N, Beavis WD, Grant D, Katt M et al. (2002) Expanding the genetic
733 map of maize with the intermated B73 x Mo17 (IBM) population. Plant molecular biology
734 48: 453-461.
735 9. Balint-Kurti PJ, Zwonitzer JC, Wisser RJ, Carson ML, Oropeza-Rosas MA et al. (2007)
736 Precise Mapping of Quantitative Trait Loci for Resistance to Southern Leaf Blight, Caused
737 by Cochliobolus heterostrophus Race O, and Flowering Time Using Advanced Intercross
738 Maize Lines. Genetics 176: 645-657.
739 10. Dubois PG, Olsefski GT, Flint-Garcia S, Setter TL, Hoekenga OA et al. (2010)
740 Physiological and Genetic Characterization of End-of-Day Far-Red Light Response in
741 Maize Seedlings. Plant Physiol 154: 173-186.
742 11. Hazen SP, Hawley RM, Davis GL, Henrissat B, Walton JD (2003) Quantitative Trait Loci
743 and Comparative Genomics of Cereal Cell Wall Composition. Plant Physiology 132: 263-
744 271.
745 12. Lung'aho MG, Mwaniki AM, Szalma SJ, Hart JJ, Rutzke MA et al. (2011) Genetic and
746 physiological analysis of iron biofortification in maize kernels. PLoS One 6: e20429.
747 13. Ordas B, Malvar RA, Santiago R, Butron A (2010) QTL mapping for Mediterranean corn
748 borer resistance in European flint germplasm using recombinant inbred lines. BMC
749 Genomics 11: 1-10.
750 14. Zhang N, Gibon Y, Gur A, Chen C, Lepak N et al. (2010) Fine Quantitative Trait Loci
751 Mapping of Carbon and Nitrogen Metabolism Enzyme Activities and Seedling Biomass in

752 the Maize IBM Mapping Population. Plant Physiology 154: 1753-1765.
753 15. Shakoor N, Ziegler G, Dilkes BP, Brenton Z, Boyles R et al. (2016) Integration of
754 experiments across diverse environments identifies the genetic determinants of variation in
755 Sorghum bicolor seed element composition. Plant physiology pp-01971.
756 16. Broman KW, Speed TP (2002) A model selection approach for the identification of
757 quantitative trait loci in experimental crosses. Journal of the Royal Statistical Society:
758 Series B (Statistical Methodology) 64: 641-656.
759 17. Churchill GA, Doerge RW (1994) Empirical threshold values for quantitative trait
760 mapping. Genetics 138: 963-971.
761 18. Millikan CR (1948) Antagonism between molybdenum and certain heavy metals in plant
762 nutrition. Nature 161: 528.
763 19. Bhatia A, Yadav A, Zhu C, Gagneur J, Radhakrishnan A et al. (2014) Yeast Growth
764 Plasticity Is Regulated by Environment-Specific Multi-QTL Interactions. G3 4: 769-777.
765 20. Leinonen PH, Remington DL, Leppälä J, Savolainen O (2013) Genetic basis of local
766 adaptation and flowering time variation in Arabidopsis lyrata. Molecular ecology 22: 709-
767 723.
768 21. Nichols KM, Broman KW, Sundin K, Young JM, Wheeler PA et al. (2007) Quantitative
769 Trait Loci x Maternal Cytoplasmic Environment Interaction for Development Rate in
770 Oncorhynchus mykiss. Genetics 175: 335-347.
771 22. Tétard-Jones C, Kertesz MA, Preziosi RF (2011) Quantitative trait loci mapping of
772 phenotypic plasticity and genotype-environment interactions in plant and insect
773 performance. Philosophical Transactions of the Royal Society of London B: Biological
774 Sciences 366: 1368-1379.

775 23. Ungerer MC, Halldorsdottir SS, Purugganan MD, Mackay TFC (2003) Genotype-
776 Environment Interactions at Quantitative Trait Loci Affecting Inflorescence Development
777 in Arabidopsis thaliana. Genetics 165: 353-365.
778 24. Des Marais DL, Hernandez KM, Juenger TE (2013) Genotype-by-environment interaction
779 and plasticity: exploring genomic responses of plants to the abiotic environment. Annual
780 Review of Ecology, Evolution, and Systematics 44: 5-29.
781 25. White JG, Zasoski RJ (1999) Mapping soil micronutrients. Field Crops Research 60: 11-26.
782 26. Godt J, Scheidig F, Grosse-Siestrup C, Esche V, Brandenburg P et al. (2006) The toxicity
783 of cadmium and resulting hazards for human health. J Occup Med Toxicol 1: 22.
784 27. United States Department of Agriculture GAIN (2014) China's Maximum Levels of
785 Contaminants in Food. GAIN report CH14058. Available:
786 http://gain.fas.usda.gov/Recent%20GAIN%20Publications/Maximum%20Levels%20of%2
787 0Contaminants%20in%20Foods%20_Beijing_China%20-
788 %20Peoples%20Republic%20of_12-11-2014.pdf via the Internet. Accessed x.
789 28. López-Arredondo DL, Leyva-González MA, González-Morales SI, López-Bucio J,
790 Herrera-Estrella L (2014) Phosphate nutrition: improving low-phosphate tolerance in crops.
791 Annual Review of Plant Biology 65: 95-123.
792 29. Lin Y-F, Liang H-M, Yang S-Y, Boch A, Clemens S et al. (2009) Arabidopsis IRT3 is a
793 zinc-regulated and plasma membrane localized zinc/iron transporter. New Phytologist 182:
794 392-404.
795 30. Mulder EG (1948) Importance of molybdenum in the nitrogen metabolism of
796 microorganisms and higher plants. Plant and Soil 1: 94-119.
797 31. Mulder EG, Gerretsen FC (1952) Soil manganese in relation to plant growth. Adv Agron 4:

221-277.

Supporting Information

S1 Fig. Variances of Principal Components from PCA within 10 Environments. Eigenvalues (amount of variation explained) for each PC are shown on the y-axis. Lines are colored by environment.

S2 Fig. Variances of Principal Components from PCA on Common Lines in Six Environments. Eigenvalues (amount of variation explained) for each PC are shown on the y-axis. PC1-7 account for 98% of total variance.

S1 Table. Growout Information.

S2 Table. Percent Variance (R^2) of Mo, Cd, and Ni QTL.

S3 Table. Location LOD Scores Compared to Seed Element Content.